Enhanced Hammerstein Behavioral Model for Broadband Wireless Transmitters

Junghwan Moon, *Student Member, IEEE*, and Bumman Kim, *Fellow, IEEE*

***Abstract*—A novel enhanced Hammerstein behavior model consisting of a weighted memoryless polynomial followed by a Volterra filter is proposed. The weighted polynomial is used for predicting the strong static nonlinear behaviors of the power amplifiers (PAs). Since the Volterra filter is employed only for the mild dynamic nonlinearities, the filter can be implemented with low nonlinear order. Thus, this proposed model is capable of predicting both the static and dynamic nonlinearities of RF PAs with the acceptable complexity. The modeling performance of the proposed model is assessed in terms of in-band and out-of-band errors, such as normalized mean square error and adjacent channel error power ratio, and it is compared with a conventional Hammerstein, an augmented Hammerstein, and a Volterra series with respect to computation complexities such as the number of floating point operations and coefficients. The excellent estimation capability of the enhanced Hammerstein model is validated by two kinds of PAs: Si lateral diffusion metal–oxide–semiconductor and GaN high electron-mobility transistor amplifiers. Furthermore, the proposed scheme is applied to the digital predistortion (DPD) to cancel the nonlinearities of the PAs. The modeling performances and DPD experimental results clearly demonstrate the superiority of the enhanced Hammerstein scheme: the computational complexity is comparable with the augmented Hammerstein behavioral model, but the modeling performance is similar to the Volterra filter, which is the most accurate model.**

***Index Terms*—Behavior modeling, Hammerstein, memory effect, power amplifier (PA), PA nonlinearity, two-box model, Volterra series, wideband behavioral model.**

I. Introduction

THE POWER amplifier (PA) is an essential element in current wireless communication systems. However, it is inherently a nonlinear component. The nonlinearity induces in-band and out-of-band error distortions that cause adjacent channel interference and degradation of bit-error-rate performance. Thus, to meet the linearity requirements mandated by regulatory agencies, it is necessary to compensate for the nonlinear characteristics of the PA. Traditionally, PAs were driven into the back-off power region, required more than peak-to-average power ratio (PAPR), to operate within the linear region. However, modern communication systems, such as wideband code-division multiple access (WCDMA) and world interoperability for microwave access (WiMAX), use spectrally efficient modulation schemes to transmit large quantities of information within a limited band. As a result, the signals of the systems vary rapidly and have a large PAPR. Thus, the PA should be operated at a power level far from its saturation point, where the dc-to-RF conversion efficiency is poor. To improve the efficiency without compromising linearity, the PA linearization technique is indispensable [1]–[5].

The feedforward linearization technique provides extremely linear and broadband characteristics [6], [7]. However, it is an expensive method, consisting of an auxiliary error amplifier and complicated control circuits. Moreover, due to the error amplifier, the overall efficiency of the system is poor. On the other hand, feedback linearization has the disadvantages of instability and bandwidth limitation [8], [9]. An analog predistortion (PD) is preferred due to its simple structure and low cost [10], [11]. Nevertheless, the linearization performance for a wideband signal is restricted. Among all linearization techniques, digital predistortion (DPD) is the most promising technique because of its high accuracy, energy-efficient operation, and flexibility; Therefore, it is widely employed [12]–[57].

The key element of the DPD is an extra nonlinear function before the PA to preprocess input signal of the PA; as a result, the overall cascaded system $(\mathrm{DPD}+\mathrm{PA})$ linearly amplifies signals. To determine the nonlinear function, a behavioral model and inverse model of PAs are needed in the DPD system. In addition, the behavioral model for the PA provides a convenient and efficient means to estimate system-level performance without the computational complexity of circuit-level simulation or physical nonlinear-circuit analysis, which speeds up the system design and verification process. Currently, many types of behavior modeling methods for memory or memoryless PAs have been proposed and evaluated. For example, the Saleh model [17], Volterra-based models [18]–[30], Wiener-based model [30]–[33], Hammerstein-based model [34]–[36], memory polynomial model [37]–[39], and neural network-based model [40]–[44]. In addition, overview and comparative analysis of the various models have been presented [45]–[47].

As radio systems evolve to use wider bandwidth signals, we have to account for not only static nonlinearities defined by amplitude modulation/amplitude modulation (AM/AM) and amplitude modulation/phase modulation (AM/PM), but also the memory effects to accurately model the PA. Memory effects

Manuscript received July 12, 2010; revised December 03, 2010; accepted December 21, 2010. Date of publication February 24, 2011; date of current version April 08, 2011. This work was supported by The Ministry of Knowledge Economy (MKE), Korea, under the Information Technology Research Center (ITRC) Support Program supervised by the National Information Technology Industry Promotion Agency (NIPA)(NIPA-2010-(C1090-1011- 0011)), by the World Class University (WCU) Program through the National Research Foundation of Korea funded by the Ministry of Education, Science and Technology (R31-2010-000-10100-0), and by the Brain Korea 21 Project in 2010.

The authors are with the Department of Electrical Engineering and the Division of Information Technology Convergence Engineering, Pohang University of Science and Technology, Pohang, Gyeongbuk 790-784, Korea (e-mail: jhmoon@postech.ac.kr; bmkim@postech.ac.kr).

Digital Object Identifier 10.1109/TMTT.2011.2110659

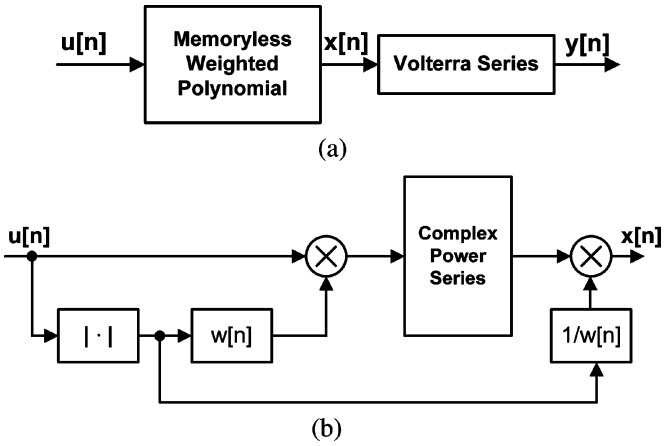

Fig. 1. Block diagrams of: (a) Enhanced Hammerstein behavior model and (b) weighted polynomial.

can generally be categorized as: 1) linear memory effects that arise from time delays or phase shifts in the PA matching circuitry and the device elements used and 2) dynamic memory effects caused by trapping effects and nonideal bias circuits [27], [48]. Several PA behavior model topologies, which are intended to describe the static nonlinearities and memory effects, have been reported in the literature. A Volterra series provides a general way to accurately model a dynamic nonlinear system by including all possible nonlinear components. However, since both the nonlinearity and memory effect are estimated simultaneously in the Volterra model, the number of the coefficients to be extracted increases rapidly with respect to degree of the nonlinearity and memory length of the system, which increases the complexity. Therefore, this model is useful for a system with a moderate degree of nonlinearity. To overcome the computational complexity of the Volterra series, Volterra-like approaches have been proposed [21]–[27]. For example, the dynamic deviation reduction-based Volterra series [27] reduces the number of coefficients by removing high-order dynamics in the classical Volterra series. However, in this Volterra series, highly nonlinear static and mildly nonlinear dynamics are identified in a single step. Thus, the generated Vandermonde matrix, which is employed in the identification process, is large, and solving the matrix is very complex [49], [50]. The memory polynomial in which all off-diagonal coefficients of the Volterra kernel are set to zero is widely used to model the PAs. However, this method often results in an oversized model due to the use of a constant nonlinear degree in all branches. Moreover, lack of the cross-term in this model limits the modeling accuracy. Two-box models, generally known as Wiener and Hammerstein models, employ a cascade of a nonlinear function and a linear filter to model the dynamic systems. These models do not consider the nonlinear behavior of the memory effect and cross-term, which limits the modeling performance. To alleviate the drawbacks of the conventional Wiener and Hammerstein structures, a weakly nonlinear block with multiple filters is employed as the memory subsystem in the augmented versions of these models [33], [36]. The twin nonlinear two-box (TNTB) models [50], in which the lookup table and memory polynomial function are placed in forward, reverse, and parallel ways, are proposed to represent the memory effect with strong static nonlinearity. In these TNTB models, the parameter identifications for both highly nonlinear static and the mildly nonlinear dynamic behavior are separately carried out. However, these models do not include the cross-term.

The behavioral models are usually compared using the number of coefficients, which determines the memory size needed for computation. However, this comparison may not always be the proper method. For example, in a neural network, the number of parameters may not accurately represent the computational complexity. Additionally, a simple approach to measure the complexity is to record the running time of the different models. However, this measure depends on the hardware setup. Recently, to fairly compare the models, Tehrani *et al.* [47] employs the number of floating point operations (FLOPs) for measuring the complexity. The computational effort mainly depends on the number of additions, subtractions, and multiplications in the field-programmable gate array or digital signal processing rather than the number of coefficients.

In this paper, an enhanced Hammerstein behavior model consisting of a cascade of a memoryless weighted polynomial, proposed in [51], followed by a Volterra series is investigated to separately model the mildly nonlinear memory effect, as well as the strongly static nonlinearity. By applying the weighting function, which includes the effect for the errors during the coefficient identification for the static nonlinear behavior due to the statistic distribution of the commonly used signal of the wireless communication system and high level of generation at the high power level, the weighted memoryless polynomial reduces the modeling error. Since a Volterra filter in the enhanced Hammerstein model is employed only for predicting the nonlinear memory effect with a mild degree of nonlinearity, the computation complexity can be reduced in comparison with the conventional Volterra series, in which the both strongly static and mildly dynamic nonlinear behavior of the PAs are modeled at once. However, in spite of the Volterra series with a low degree of nonlinearity, performance of the proposed model is similar to that of the conventional Volterra series. The proposed model is compared with the Hammerstein-based models, such as conventional and augmented Hammerstein structures, and Volterra series in terms of normalized mean square error (NMSE) and adjacent channel error power ratio (ACEPR) as a function of the number of total coefficients and FLOPs. Additionally, the enhanced Hammerstein predistorter constructed by the indirect learning architecture is designed to validate the effectiveness of such a predistorter. The linearization performance of this predistorter is compared with the augmented Hammerstein architecture. The modeling and linearization performances clearly show that the proposed model provides excellent results.

This paper is organized as follows. First, the proposed model is described in Section II. The modeling performance is then assessed in Section III. In Section IV, the experimental results of a baseband digital predistorter based on the proposed models are presented. Finally, conclusions are presented in Section V.

II. Enhanced Hammerstein Behavioral Model

The enhanced Hammerstein behavioral model, illustrated in Fig. 1(a), consists of a memoryless sub-block followed by a dynamic nonlinear system. To model the static nonlinear behaviors of the PAs, such as AM/AM and AM/PM, the memoryless weighted polynomial model, which is proposed and well described in [51], is employed, as shown in Fig. 1(b). This model consists of weighting, polynomial to the error signal, and de-weighting parts. By applying the weighting function, presenting the statistical distribution of the signal and emphasizing the high power level, this polynomial delivers higher modeling accuracy than the conventional polynomial.

To predict the mildly dynamic memory effects of the PAs, a Volterra filter is adopted. In general, a discrete time-domain finite-memory complex baseband Volterra model is given by

$$y(n) = \sum_{p=1}^{P} y_p(n) \tag{1}$$

where

$$y_p(n) = \begin{cases} \sum\limits_{i=0}^{N_p-1} h_{(p)}(i)x(n-i), & \text{for } p=1 \\ \sum\limits_{i_1=0}^{N_p-1} \cdots \sum\limits_{i_p=0}^{N_p-1} h_{(p)}(i_1,\ldots,i_p) \\ \quad \times \prod\limits_{k=1}^{(p+1)/2} x(n-i_k) \\ \quad \times \prod\limits_{k=(p+3)/2}^{p} x^*(n-i_k), & \text{for } p>1, \text{ odd.} \end{cases} \tag{2}$$

$x(n)$ and $y(n)$ are input and output of the Volterra filter, respectively. N_p represents the memory depth of the corresponding nonlinearity, $h_{(p)}(i_1,\ldots,i_p)$ is the pth-order Volterra kernel, and P is the nonlinear degree of this model. In this study, we have considered only the second-order cross terms, i.e., the products with two different time delays. Moreover, even-order terms are included to enrich the basis set and improve the modeling accuracy and DPD performance [52]. With the above considerations, the Volterra model is approximated by a simplified model, described in [28], given by

$$y_p(n) = \begin{cases} \sum\limits_{i=0}^{N_p-1} h_i^{(p)} x(n-i), & \text{for } p=1 \\ \sum\limits_{i=0}^{N_p-1} \sum\limits_{j=0}^{N_p-1} h_{ij}^{(p)} x(n-i)|x(n-j)|^{p-1}, & \text{for } p>1. \end{cases} \tag{3}$$

In the remainder of this paper, we use the Volterra series in (3) not only for the validation of the enhanced Hammerstein model, but also for that of the Volterra model instead of the classical version.

Since the Volterra model in the enhanced Hammerstein behavior model is used only for estimating the mildly nonlinear behavior of memory effects, the nonlinear degree of the model can be significantly reduced in comparison with the model used for predicting both static and dynamic nonlinearities. Thus, the total number of the coefficients and computational complexity

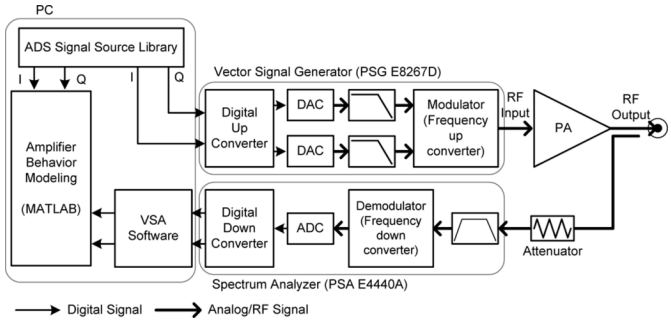

Fig. 2. Experimental setup used to evaluate the behavioral model and DPD.

are reduced. Since this model uses the dynamic nonlinearity with a high order to predict the nonlinear memory effects, it can deliver better modeling performance than the conventional Hammerstein structure with a linear filter expressed as

$$y(n) = \sum_{i=1}^{M_1-1} a_i x(n-i). \tag{4}$$

The augmented Hammerstein and TNTB models alleviate the drawback of the conventional Hammerstein by employing the nonlinearity of the memory effect, given by

$$y(n) = \sum_{i=1}^{M_1-1} a_i x(n-i) + \sum_{i=1}^{M_2-1} b_i x(n-i)|x(n-i)| \tag{5}$$

$$y(n) = \sum_{j=0}^{M_1-1} \sum_{i=1}^{N} a_{j,i} x(n-j)|x(n-j)|^{i-1}. \tag{6}$$

Equations (5) and (6) denote the memory subsystems for the augmented Hammerstein and TNTB, respectively. However, the cross-terms between the previous input signals are not included in the memory-effect model, which limits the modeling accuracy.

The identification procedure employed in the proposed model consists of two steps. Initially, the static nonlinear behavior is extracted by the memoryless weighted polynomial. The dynamic nonlinearity of the PAs is then de-embedded from the data of the amplifier output. Next, the coefficients of the Volterra filter are identified. This separated identification procedure reduces the size of the Vandermonde matrix compared to the dynamic deviation reduction-based Volterra series. However, compared to an unique identification, a two-step identification is less stable for the local minimum problem. Thus, during the identification phase, a careful adaptation is required.

In short, the enhanced Hammerstein structure consists of a weighted memoryless polynomial to model the high-order static nonlinearity and the Volterra filter to predict the relatively small nonlinear-memory effect. Therefore, the number of coefficients and FLOPs can be reduced compared to the Volterra approach in which both the static and dynamic nonlinearities are modeled simultaneously. Compared to the conventional Hammerstein, conventional Wiener with the separated identification, their augmented versions, and TNTB models, the modeling performance is improved by including the cross-terms to accurately model the memory effect.

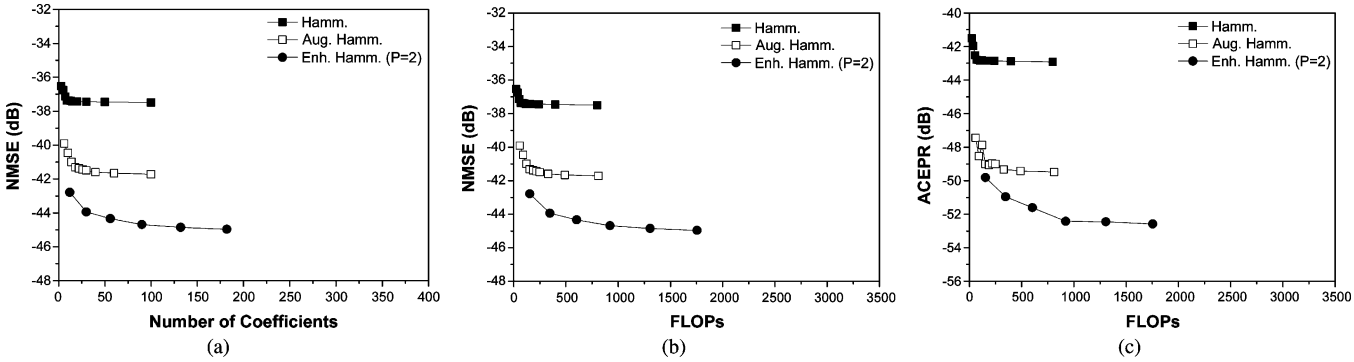

Fig. 3. Case-I: Class-AB amplifier using Si LDMOSFET at an average output power back-off of 8 dB. (a) NMSE values according to the total number of coefficients. (b) NMSE and (c) ACEPR according to FLOPs.

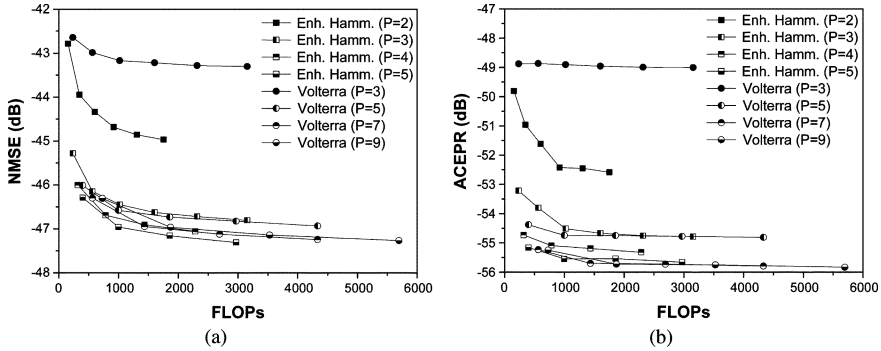

Fig. 4. Case-I: Class-AB amplifier using Si LDMOSFET at an average output power back-off of 8 dB. (a) NMSE and (b) ACEPR comparisons between enhanced Hammerstein and Volterra models according to the total number of FLOPs.

III. Enhanced Hammerstein Model Validation

The ability of the enhanced Hammerstein model to predict the responses of PAs is compared with the conventional Hammerstein, augmented Hammerstein, and Volterra series. The Volterra series used for the comparison is the same form in the enhanced Hammerstein, as described in (1) and (3). All models considered in this section include even- as well as odd-degree nonlinearities to increase modeling accuracy [52].

A. Measurement Setup

The experimental setup used to evaluate the behavior model and DPD is shown in Fig. 2. An Agilent E4438C electronic signal generator (ESG) was used as the modulator, and a 89600 vector signal analyzer (VSA) was used as a demodulator. The baseband in-phase/quadrature (I/Q) data were generated in a computer and downloaded to ESG; the data were modulated to an RF carrier. The resulting signal was fed to the PA. The output signal of the PA was then captured by the E4440A PSA, and the output I/Q data were collected by the VSA [53]. The behavioral model and its inversion were carried out by MATLAB.

For comprehensive validation, performances of the enhanced Hammerstein and other models are evaluated in two kinds of Class-AB amplifiers. The first Class-AB PA is implemented using 140-W Si lateral diffusion metal–oxide–semiconductor (LDMOSFET) at 2.345 GHz, and the second one is designed using 120-W GaN high electron-mobility transistor (HEMT) at 2.655 GHz. For the LDMOSFET amplifier, a WCDMDA two frequency assignment (2FA) signal with a carrier spacing of 10 MHz is applied. The signal has a PAPR of 8 dB and a bandwidth of 15 MHz. The output I/Q data of the amplifier is collected at the different output power levels: 8- and 6-dB back-off power conditions from the maximum output power. For the GaN HEMT amplifier, a WiMAX 2FA signal with a PAPR of 8 dB and a bandwidth of 20 MHz is used, and the output I/Q signal is gathered at the 8-dB back-off power level. For clarity, the experimental conditions are listed as follows.

- **Case-I:** Class-AB PA using Si LDMOSFET at an average output power back-off of 8 dB.
- **Case-II:** Class-AB PA using GaN HEMT at an average output power back-off of 8 dB.
- **Case-III:** Class-AB PA using Si LDMOSFET at an average output power back-off of 6 dB.

B. Model Evaluation Metrics

Many performance measures to validate behavioral models have been reported, e.g., NMSE [18], root mean square error [54], ACEPR [55], memory effect ratio, memory effect modeling ratio [56], and memory effect intensity [57]. Among them, the NMSE is adopted as the in-band model measure in this study [47], which is defined as

$$\mathrm{NMSE} = \frac{\sum_{n=1}^{M} |y_{\mathrm{PA}}(n) - \widetilde{y}(n)|^2}{\sum_{n=1}^{M} |y_{\mathrm{PA}}(n)|^2} \tag{7}$$

where y_{PA} and $\widetilde{y}$ denote the measured and modeled signals, respectively, and M is the total number of samples used to validate

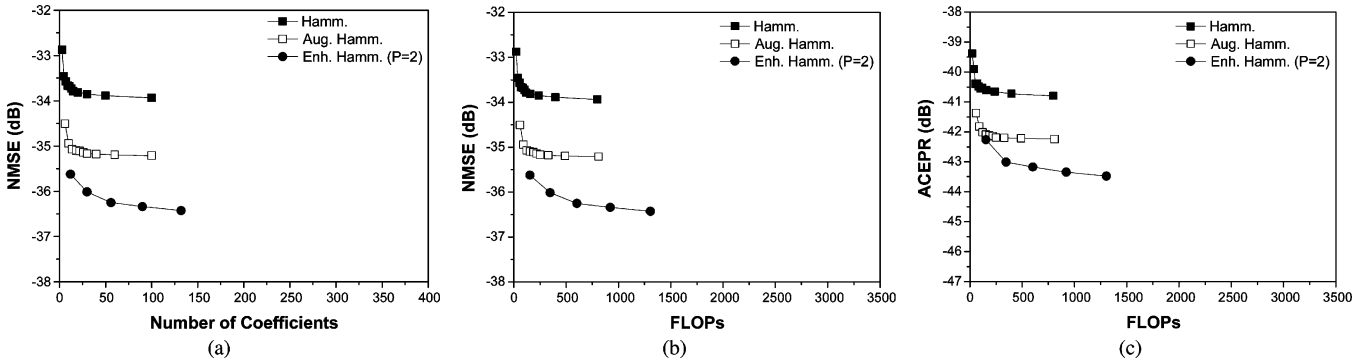

Fig. 5. Case-II: Class-AB amplifier using GaN HEMT at an average output power back-off of 8 dB. (a) NMSE values according to the total number of coefficients. (b) NMSE and (c) ACEPR according to FLOPs.

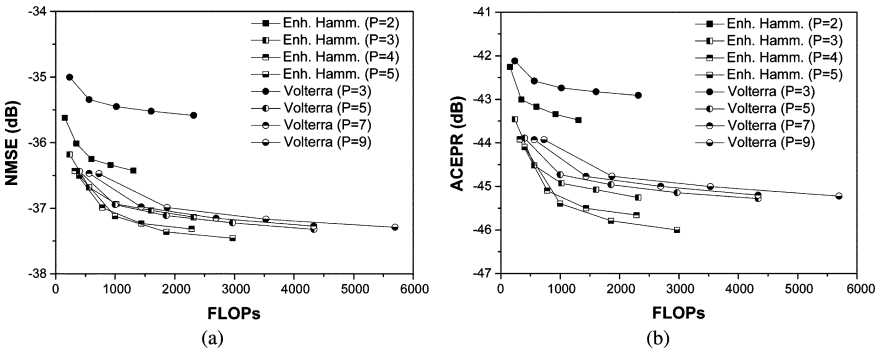

Fig. 6. Case-II: Class-AB amplifier using GaN HEMT at an average output power back-off of 8 dB. (a) NMSE and (b) ACEPR comparison between enhanced Hammerstein and Volterra models according to the total number of FLOPs.

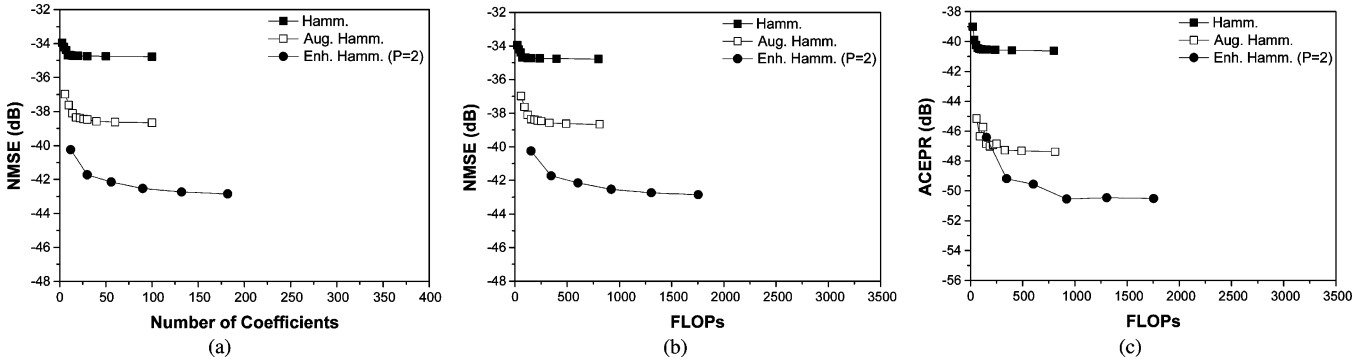

Fig. 7. Case-III: Class-AB amplifier using Si LDMOSFET at an average output power back-off of 6 dB. (a) NMSE values according to the total number of coefficients. (b) NMSE and (c) ACEPR according to FLOPs.

the models. To assess the out-of-band modeling capability, the ACEPR is used and defined as

$$\mathrm{ACEPR} = \max_{m=1,2} \left\{ \frac{\int_{(\mathrm{adj})_m} |Y_{\mathrm{PA}}(f) - \widetilde{Y}(f)|^2}{\int_{\mathrm{ch}} |Y_{\mathrm{PA}}(f)|^2} \right\} \quad (8)$$

where Y_{PA} and $\widetilde{Y}$ are Fourier transforms of the measured and modeled data, respectively. The integration in the denominator is over the in-band channel, and the integration in the numerator is from the adjacent channels to the signal channel with the same bandwidth for the lower $(m = 1)$ and upper $(m = 2)$ adjacent channels.

C. Results

The modeling performances of the conventional Hammerstein, augmented Hammerstein, enhanced Hammerstein, and Volterra models are assessed in terms of NMSE and ACEPR according to the computational complexity. In order to represent the static nonlinear behaviors of the conventional, augmented, and enhanced Hammerstein models, the memoryless polynomials are employed. For Case-I, Case-II, and Case-III, the polynomial orders are set to 7, 5, and 7, respectively. The memory depth of the conventional Hammerstein M_1 is changed from 3 to 100. For the augmented case, M_1 and M_2 are swept from 3 to 50, respectively. In the enhanced Hammerstein, the nonlinear degree P and memory depth N_p of the Volterra series are varied from 2 to 5 and 3 to 13, respectively. For the Volterra series, it predicts the dynamics, as well as static nonlinear behavior at once. Thus, its polynomial order is swept from 3 to 9, and memory depth is changed from 3 to 13. When calculating these metrics, 20 000 input and output I/Q samples for both the WCDMA 2FA and WiMAX 2FA signals are employed. For the

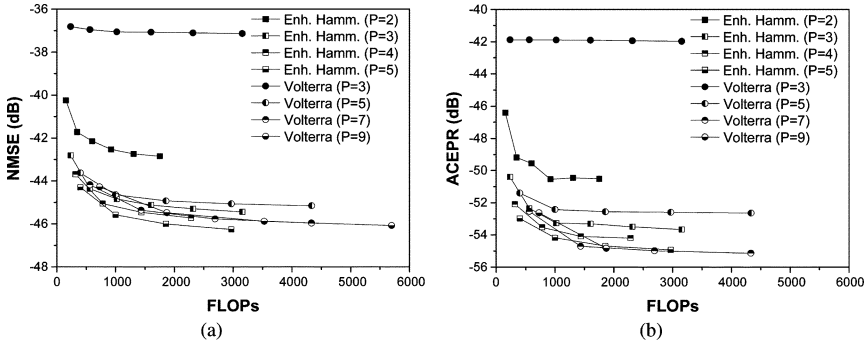

Fig. 8. Case-III: Class-AB amplifier using Si LDMOSFET at an average output power back-off of 6 dB. (a) NMSE and (b) ACEPR comparison between enhanced Hammerstein and Volterra models according to the total number of FLOPs.

complexity measure, the number of FLOPs is employed, and the total number of FLOPs is calculated using (1) and (3)–(5) [47].

1) Case-I: Figs. 3 and 4 show comparisons of the NMSE and ACEPR for the behavioral models with respect to the total number of coefficients and FLOPs. In Fig. 3, the modeling performances of the proposed model are compared with those of Hammerstein and its augmented version. The performance of the Volterra series is also evaluated and depicted in Fig. 4. "P" in the legends for the enhanced Hammerstein and Volterra series denotes the nonlinear degree of the Volterra series. From Fig. 3, it can be seen that as the calculation resources, such as the total number of coefficients and FLOPs, increase, the NMSE and ACEPR performances improve. However, the minimum levels of the models are limited for each algorithm used. For the Hammerstein model, the NMSE and ACEPR are limited to -37.4 and -42.9 dB, respectively, because this algorithm employs only a linear filter to model the memory effect. On the other hand, the augmented Hammerstein gives better performances than the classical Hammerstein. The minimum NMSE and ACEPR of the augmented Hammerstein are -41.7 and -49.4 dB, respectively, because the augmented Hammerstein includes the second-degree nonlinear characteristic of the memory effect. For the enhanced Hammerstein with a nonlinear degree of 2, which is the same degree of the augmented Hammerstein case, the performances are further improved over the Hammerstein models. The minimum NMSE and ACEPR of the enhanced Hammerstein are -44.9 and -52.6 dB, respectively. This result indicates that the cross-term is important to characterize the memory effect. The proposed model converges accurately, providing better accuracy than other models with fewer than 500 FLOPs.

The enhanced Hammerstein and the Volterra series have been compared extensively, as shown in Fig. 4. Unlike the Volterra series, in which the memoryless nonlinearity and memory effect are predicted at once, the proposed model delivers better in-band and out-of-band modeling performances with a low nonlinear degree because the static and dynamic nonlinear behaviors of the PAs are estimated independently. For both behavioral models, the lowest NMSE and ACEPR are similar when the number of coefficients and FLOPs are large. However, at a finite complexity, the proposed model delivers lower NMSE error than that of the Volterra filter.

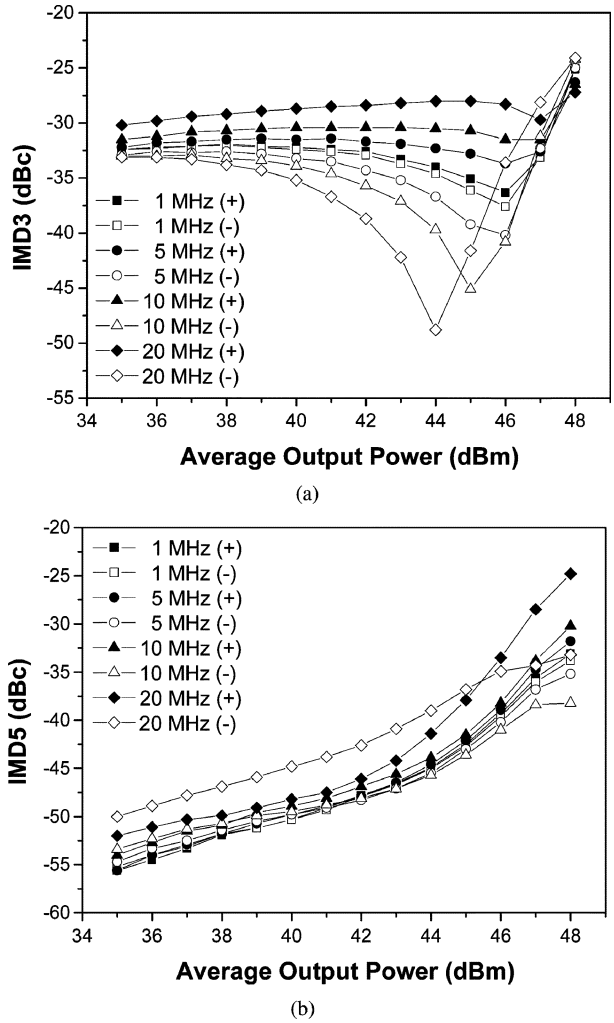

Fig. 9. Measured: (a) IMD3 and (b) IMD5 characteristics.

2) Case-II: In this case, we explore the nonlinear behavior of the Class-AB PA using GaN HEMT with a signal bandwidth of 20 MHz. Fig. 5 shows the modeling performances for the Hammerstein, augmented Hammerstein, and enhanced Hammerstein. Although the enhanced Hammerstein model outperforms the others, the performance differences of all models are relatively small because the GaN HEMT generates less memory effect than Si LDMOSFET because of the

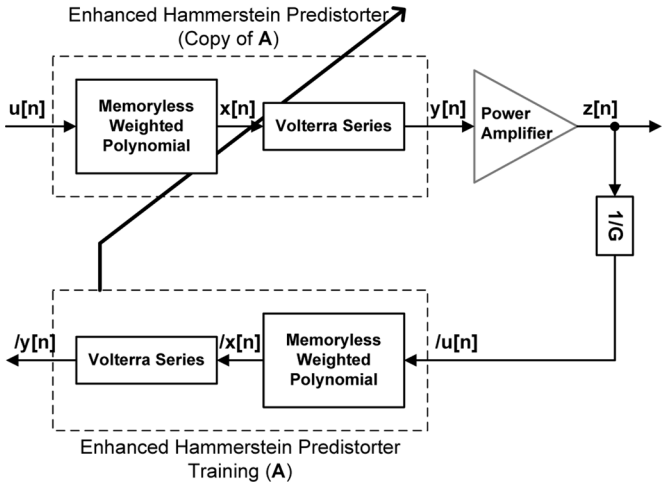

Fig. 10. Offline training scheme for enhanced Hammerstein predistorter identification.

large impedance level. Therefore, the models do not show any significant improvement from the static nonlinear model, which delivers −31.8 dB of NMSE. In Fig. 6, the enhanced Hammerstein and Volterra series are compared with respect to the number of FLOPs. Unlike Case-I, there is no significant improvement as the polynomial order increases, which indicates that the nonlinear degree of the memory effect is mild for the GaN HEMT. These evaluations show again that the proposed behavioral modeling has the outstanding capability to predict PA behavior that exhibits the memory effect regardless of device and signal bandwidth.

3) Case-III: The Class-AB PA used in Case-I is driven harder in this case, and the PA has more static and dynamic nonlinear characteristics. Thus, compared with Case-I, the modeling accuracy is slightly degraded. In Figs. 7 and 8, the modeling performances are compared with respect to the number of coefficients and FLOPs. Similar to the previous cases, the enhanced Hammerstein model delivers the lowest modeling error among NMSE and ACEPR, as shown in Fig. 7. Moreover, the amount of improvement between the augmented and enhanced Hammerstein models is increased in comparison with Case-I, which proves that the proposed model can predict the memory effect with complex behavior. In Fig. 8, the modeling performances of the Volterra series are compared with those of the proposed model. Due to the harder saturation characteristic than Case-I, the amount of improvement for NMSE is slightly increased from 1.8 to 2.6 dB when the polynomial order of the Volterra filter in the enhanced Hammerstein is increased from 2 to 3. Similarly to Case-I, the lowest NMSE and ACEPR values of both enhanced Hammerstein and Volterra models are nearly the same. However, at a finite complexity, the proposed model provides lower NMSE error than that of the Volterra model, but ACEPR performances for both models are similar.

4) Discussion: The modeling performances of the Hammerstein-kind models are compared, and the proposed enhanced Hammerstein model has the best performance, which is similar to that of the Volterra series. If infinite resources are given, the proposed model can achieve the best in-band and out-of-band modeling performance compared to the Hammerstein kinds of models for various PAs and saturation levels. With lower computational complexity, such as fewer coefficients and FLOPs, the enhanced Hammerstein can provide similar performance to the Volterra series.

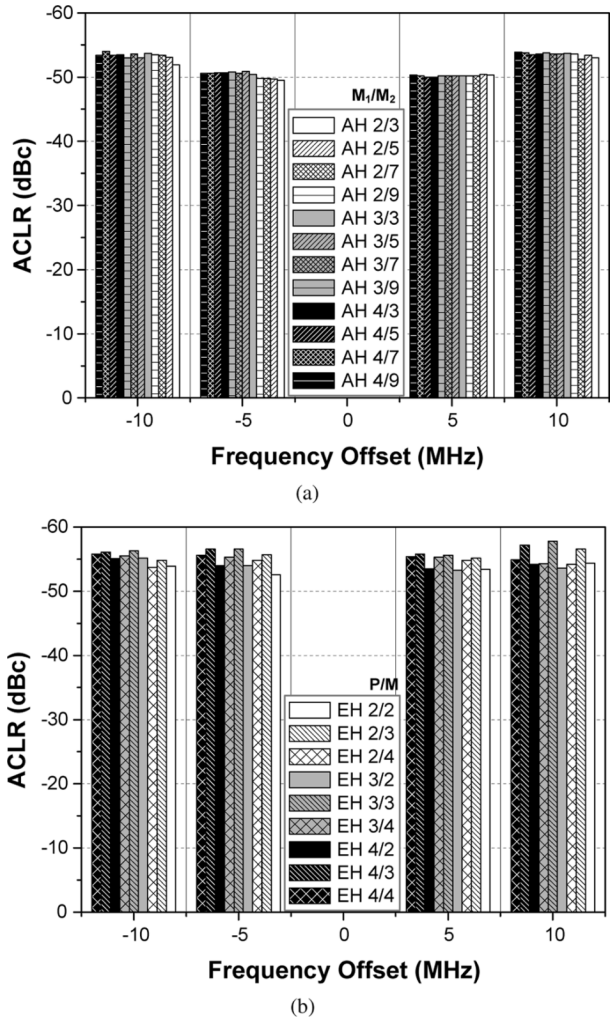

Fig. 11. ACLR comparisons of the transmitter with different parameters for WCDMA 4FA signal. (a) Augmented Hammerstein with two different delay-tap FIR filters. (b) Enhanced Hammerstein with the various polynomial orders and delay-tap.

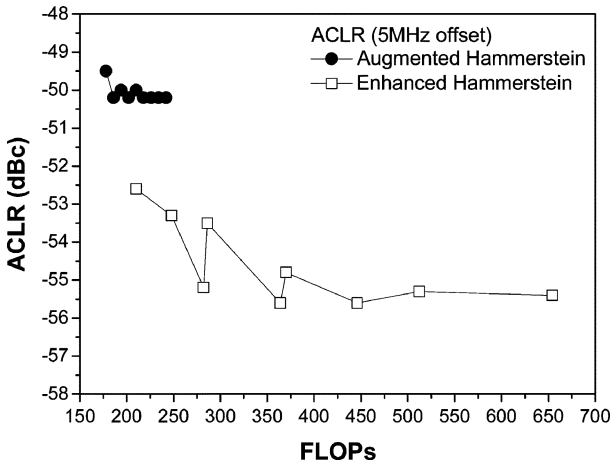

Fig. 12. ACLRs of the augmented and enhanced Hammerstein predistorters according to the number of FLOPs.

TABLE I
SUMMARY OF THE DPD LINEARIZATION RESULTS AT AN AVERAGE OUTPUT POWER OF 42 dBm

Model	Coeff.	FLOPs	ACLR [dBc]			
			+5 MHz	–5 MHz	+10 MHz	–10 MHz
Amplifier	–	–	–33.5	–38.1	–34.9	–41.6
Memoryless Ploynomial	12	128	–46.6	–45.3	–46.3	–44.1
Augmented Hammerstein ($M_1 = 3,\ M_2 = 9$)	23	234	–50.2	–50.8	–53.8	–53.0
Enhanced Hammerstein ($P = 2,\ M = 3$)	23	272	–55.2	–55.7	–56.6	–54.8
Enhanced Hammerstein ($P = 3,\ M = 3$)	32	364	–55.6	–56.6	–57.8	–56.3

IV. DPD LINEARIZATION

A. PA Characteristics

The proposed enhanced Hammerstein behavioral model is applied to the DPD architecture for the pre-compensation of nonlinear distortions and memory effects in an RF PA and transmitter. To validate effectiveness of this predistorter, we built a Class-AB PA using the Freescale MRF6S21100 LDMOSFET with 100-W PEP at 2.14 GHz. The biases of the PA were set to $V_{\rm DS} = 28$ V and $I_{\rm DS} = 458$ mA. The PA has an efficiency of 48.5% and a power gain of 11.5 dB at $P_{\rm 1dB}$ of 49.8 dBm. The implemented PA is not the same amplifier used in Section III, which verifies that the proposed model can be applied to any kinds of amplifiers.

Before applying the PD algorithm, we have explored the nonlinear characteristics and memory effects using two-tone signals up to 20-MHz tone spacing. Fig. 9 shows the third-order intermodulation distortion (IMD3) and fifth-order intermodulation distortion (IMD5) for the two-tone signal. This amplifier has serious high-order memory effects, as can be seen from the differences between the upper and lower sidebands of IMD3 (greater than 6-dB difference at average output powers from 40 to 46 dBm). Unlike the IMD3 characteristics, there are no significant asymmetries in the IMD5s, which means that the amplifier generates a serious memory effect near the signal band.

B. Results

To validate the proposed DPD algorithm to linearize a wideband signal, a 2.14-GHz forward-link WCDMA 4FA signal is employed. This signal has a PAPR of 7.1 dB and a sampling rate of 92.16 million samples per second. An indirect learning architecture is employed to adjust the coefficients of the enhanced Hammerstein predistorter, as shown in Fig. 10. To illustrate the superior accuracy of the proposed DPD scheme, the spectrum and adjacent channel leakage ratio (ACLR) results are compared with those of the augmented Hammerstein predistorter. To compensate for the memoryless nonlinearity, such as AM/AM and AM/PM, the same weighted memoryless polynomial is used for both the augmented and enhanced Hammerstein DPD schemes.

The ACLR comparison results shown in Fig. 11 indicate that the enhanced Hammerstein predistorter can suppress the memory effects of the PA more effectively than the augmented Hammerstein scheme. Fig. 12 shows the ACLR performances with respect to the computational complexity, i.e., FLOPs. The enhanced Hammerstein predistorter provides improved ACLR performances across the whole FLOPs regions, more than 2-dB improvement. Table I summarizes the DPD linearization results when each DPD algorithm provides the best result, and the corresponding spectrums are depicted in Fig. 13. These experimental results clearly show that the proposed DPD algorithm, consisting of the weighted memoryless polynomial followed by the Volterra filter, can far more effectively compensate for both the static and dynamic nonlinearities of the PA than the augmented Hammerstein predistorter with comparable computational complexity.

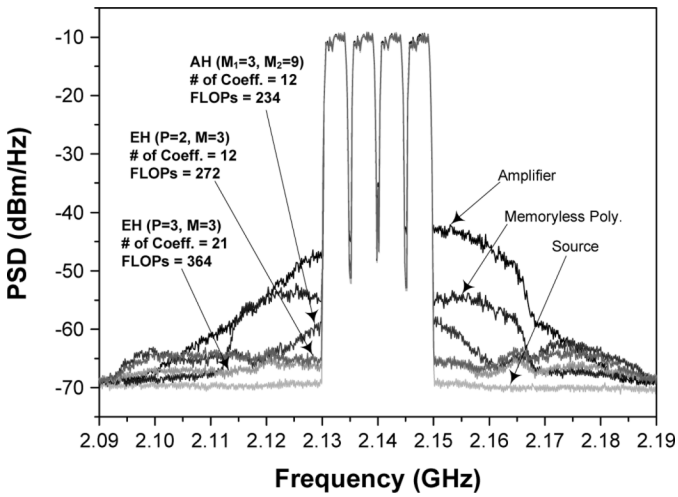

Fig. 13. Spectrum comparisons for WCDMA 4FA signal.

V. CONCLUSION

In this paper, an enhanced Hammerstein behavioral model consisting of a weighted memoryless polynomial followed by a Volterra filter has been employed to model and compensate for the distortion of PAs exhibiting the memory effect. By adopting the Volterra series as a dynamic subsystem, both linear and nonlinear memory effects can be predicted well. The cross-term of the Volterra structure improves the modeling performances. The proposed behavioral model is compared with others, such as the classical Hammerstein, augmented Hammerstein, and Volterra series, in terms of the NMSE and ACEPR with respect to the computational complexity. The results of the modeling assessment clearly show that the enhanced Hammerstein behavior model outperforms the conventional and augmented Hammerstein architectures. Compared with the Volterra series, the proposed model can deliver the comparable performance with lower complexity. The proposed structure is applied to the DPD linearization, and the excellent linearization performance is demonstrated for the four-carrier WCDMA signal.

REFERENCES

[1] F. H. Raab, P. Asbeck, S. Cripps, P. B. Kenington, Z. B. Popović, N. Pothecary, J. F. Sevic, and N. O. Sokal, "Power amplifiers and transmitters for RF and microwave," *IEEE Trans. Microw. Theory Tech.*, vol. 50, no. 3, pp. 814–826, Mar. 2002.

[2] P. B. Kenington, *High-Linearity RF Amplifier Design*. Boston, MA: Artech House, 2000.

[3] P. B. Kenington, "Linearized transmitters: An enabling technology for software defined radio," *IEEE Commun. Mag.*, vol. 40, no. 2, pp. 156–162, Feb. 2002.

[4] S. C. Cripps, *RF Power Amplifiers for Wireless Communications*, 2nd ed. Norwood, MA: Artech House, 2006.

[5] J. Choi, D. Kang, D. Kim, J. Park, B. Jin, and B. Kim, "Power amplifiers and transmitters for next generation mobile handset," *J. Semiconduct. Technol. Sci.*, vol. 9, no. 4, pp. 14–23, Dec. 2009.

[6] Y. Y. Woo, Y. Yang, J. Yi, J. Nam, J. Cha, and B. Kim, "Feedforward amplifier for WCDMA base stations with a new adaptive control method," in *IEEE MTT-S Int. Microw. Symp. Dig.*, Jun. 2002, pp. 769–772.

[7] Y. Yang, Y. Y. Woo, and B. Kim, "Optimization for error-canceling loop of the feedforward amplifier using a new system-level mathematical model," *IEEE Trans. Microw. Theory Tech.*, vol. 51, no. 2, pp. 475–482, Feb. 2003.

[8] M. R. Moazzam and C. S. Aitchison, "A low third order intermodulation amplifier with harmonic feedback circuitry," in *IEEE MTT-S Int. Microw. Symp. Dig.*, Jun. 1996, vol. 2, pp. 827–830.

[9] Y. Kim, Y. Yang, S. Kang, and B. Kim, "Linearization of 1.85 GHz amplifier using feedback predistortion loop," in *IEEE MTT-S Int. Microw. Symp. Dig.*, Jun. 1998, pp. 1678–1678.

[10] J. Yi, Y. Yang, M. Park, W. Kang, and B. Kim, "Analog predistortion linearizer for high power RF amplifier," *IEEE Trans. Microw. Theory Tech.*, vol. 48, no. 12, pp. 2709–2713, Dec. 2000.

[11] J. Cha, J. Yi, J. Kim, and B. Kim, "Optimum design of a predistortion RF power amplifier for multi-carrier WCDMA applications," *IEEE Trans. Microw. Theory Tech.*, vol. 52, no. 2, pp. 655–663, Feb. 2004.

[12] H.-H. Chen, C.-H. Lin, P.-C. Huang, and J.-T. Chen, "Joint polynomial and look-up-table predistortion power amplifier linearization," *IEEE Trans. Circuits Syst. II, Exp. Briefs*, vol. 53, no. 8, pp. 612–616, Aug. 2006.

[13] S. D. Muruganathan and A. B. Sesay, "A QRD-RLS-based predistortion scheme for high-power amplifier linearization," *IEEE Trans. Circuits Syst. II, Exp. Briefs*, vol. 53, no. 10, pp. 1108–1112, Oct. 2006.

[14] H. Koeppl and P. Singerl, "An efficient scheme for nonlinear modeling and predistortion in mixed-signal systems," *IEEE Trans. Circuits Syst. II, Exp. Briefs*, vol. 53, no. 12, pp. 1368–1372, Dec. 2006.

[15] L. Ding, Z. Ma, D. R. Morgan, M. Zierdt, and G. T. Zhou, "Compensation of frequency-dependent gain/phase imbalance in predistortion linearization systems," *IEEE Trans. Circuits Syst. I, Reg. Papers*, vol. 55, no. 1, pp. 390–397, Jan. 2008.

[16] M. M. Sahbany and P. P. G. Gulak, "Efficient compensation of the nonlinearity of solid-state power amplifiers using adaptive sequential Monte Carlo methods," *IEEE Trans. Circuits Syst. I, Reg. Papers*, vol. 55, no. 10, pp. 3270–3283, Nov. 2008.

[17] A. Saleh, "Frequency-independent and frequency-dependent nonlinear models of TWT amplifiers," *IEEE Trans. Commun.*, vol. COM-29, no. 11, pp. 1715–1720, Nov. 1981.

[18] C. Eun and E. J. Powers, "A new Volterra predistorter based on the indirect learning architecture," *IEEE Trans. Signal Process.*, vol. 45, no. 1, pp. 223–227, Jan. 1997.

[19] A. Zhu and T. J. Brazil, "Behavioral modeling of RF power amplifiers based on pruned Volterra series," *IEEE Microw. Wireless Compon. Lett.*, vol. 14, no. 12, pp. 563–565, Dec. 2004.

[20] A. Zhu and T. J. Brazil, "An overview of Volterra series based behavioral modeling of RF/microwave power amplifiers," in *Proc. Wireless Microw. Technol. Conf.*, 2006, pp. 1–5.

[21] F. Filicori and G. Vannini, "Mathematical approach to large-signal modeling of electron devices," *Electron. Lett.*, vol. 27, no. 4, pp. 357–359, Apr. 1991.

[22] D. Mirri, G. Iuculano, F. Filicori, G. Pasini, G. Vannini, and G. P. Gualtieri, "A modified Volterra series approach for nonlinear dynamic systems modeling," *IEEE Trans. Circuits Syst. I, Fundam. Theory Appl.*, vol. 49, no. 8, pp. 1118–1128, Aug. 2002.

[23] D. Mirri, F. Filicori, G. Iuculano, and G. Pasini, "A nonlinear dynamic model for performance analysis of large-signal amplifiers in communication systems," *IEEE Trans. Instrum. Meas.*, vol. 53, pp. 341–350, Apr. 2004.

[24] A. Zhu and T. J. Brazil, "An adaptive Volterra predistorter for the linearization of RF high power amplifiers," in *IEEE MTT-S Int. Microw. Symp. Dig.*, Jun. 2002, pp. 461–464.

[25] A. Zhu, M. Wren, and T. J. Brazil, "An efficient Volterra-based behavioral model for wideband RF power amplifiers," in *IEEE MTT-S Int. Microw. Symp. Dig.*, Jun. 2003, pp. 787–790.

[26] A. Zhu and T. J. Brazil, "Behavioral modeling of RF power amplifiers based on pruned Volterra series," *IEEE Microw. Wireless Compon. Lett.*, vol. 14, no. 12, pp. 563–565, Dec. 2004.

[27] A. Zhu, J. C. Pedro, and T. J. Brazil, "Dynamic deviation reduction-based Volterra behavioral modeling of RF power amplifiers," *IEEE Trans. Microw. Theory Tech.*, vol. 54, no. 12, pp. 4323–4332, Dec. 2006.

[28] N. Safari, T. Røste, P. Fedorenko, and J. S. Kenny, "An approximation of Volterra series using delay envelopes, applied to digital predistortion of RF power amplifiers with memory effects," *IEEE Microw. Wireless Compon. Lett.*, vol. 18, no. 2, pp. 115–117, Feb. 2008.

[29] J. Mathews and G. L. Sicuranza, *Polynomial Signal Processing*. New York: Wiley, 2000.

[30] M. Schetzen, *The Volterra and Wiener Theories of Nonlinear Systems*. Melbourne, FL: Krieger, 2006.

[31] C. J. Clark, G. Chrisikos, M. S. Muha, A. A. Moulthrop, and C. P. Silva, "Time-domain envelope measurement technique with application to wideband power amplifier modeling," *IEEE Trans. Microw. Theory Tech.*, vol. 46, no. 12, pp. 2531–2540, Dec. 1998.

[32] H. Ku, M. D. Mckinley, and J. S. Kenney, "Extraction of accurate behavioral models for power amplifiers with memory effects using two-tone measurements," in *IEEE MTT-S Int. Microw. Symp. Dig.*, Jun. 2002, vol. 1, pp. 139–142.

[33] T. Liu, S. Boumaiza, and F. M. Ghannouchi, "Deembedding static nonlinearities and accurately identifying and modeling memory effects in wideband RF transmitters," *IEEE Trans. Microw. Theory Tech.*, vol. 53, no. 11, pp. 3578–3587, Nov. 2005.

[34] L. Ding, R. Raich, and G. T. Zhou, "A Hammerstein predistortion linearization design based on the indirect learning architecture," in *Int. Acoust., Speech, Signal Process. Conf.*, May 2002, vol. 3, pp. 2689–2692.

[35] M. E. Gadringer, D. Silveira, and G. Magerl, "Efficient power amplifier identification using modified parallel cascade Hammerstein models," in *IEEE Radio Wireless Symp. Dig.*, Jan. 2007, pp. 305–308.

[36] T. Liu, S. Boumaiza, and F. M. Ghannouchi, "Augmented Hammerstein predistorter for linearization of broadband wireless transmitters," *IEEE Trans. Microw. Theory Tech.*, vol. 54, no. 4, pp. 1340–1349, Apr. 2006.

[37] L. Ding, G. T. Shou, D. R. Morgan, Z. Ma, J. S. Kenney, J. Kim, and C. R. Giardina, "A robust digital baseband predistorter constructed using memory polynomial," *IEEE Trans. Commun.*, vol. 52, no. 1, pp. 159–165, Jan. 2004.

[38] J. Kim and K. Konstantinou, "Digital predistortion of wideband signals based on power amplifier model with memory," *Electron. Lett.*, vol. 37, no. 23, pp. 1417–1418, Nov. 2001.

[39] D. R. Morgan, Z. Ma, J. Kim, M. G. Zierdt, and J. Pastalan, "A generalized memory polynomial model for digital predistortion of RF power amplifiers," *IEEE Trans. Signal Process.*, vol. 54, no. 10, pp. 3852–3860, Oct. 2006.

[40] M. Ibnkahla, J. Sombria, F. Castanie, and N. J. Bershad, "Neural networks for modeling nonlinear memoryless communication channels," *IEEE Trans. Commun.*, vol. 45, no. 7, pp. 768–771, Jul. 1997.

[41] J. J. Xu, M. C. E. Yagoub, R. Ding, and Q. J. Zhang, "Neural-based dynamic modeling of nonlinear microwave circuits," *IEEE Trans. Microw. Theory Tech.*, vol. 50, no. 12, pp. 2769–2780, Dec. 2002.

[42] T. Liu, S. Boumaiza, and M. Ghannouchi, "Dynamic behavioral modeling of 3G power amplifiers using real-valued time-delay neural networks," *IEEE Trans. Microw. Theory Tech.*, vol. 52, no. 3, pp. 1025–1033, Mar. 2004.

[43] J. Wood, D. E. Root, and N. B. Tufillaro, "A behavioral modeling approach to nonlinear model-order reduction for RF/microwave ICs and systems," *IEEE Trans. Microw. Theory Tech.*, vol. 52, no. 9, pp. 2274–2284, Sep. 2004.

[44] M. Isaksson, D. Wisell, and D. Ronnow, "Wide-band dynamic modeling of power amplifiers using radial basis function neural networks," *IEEE Trans. Microw. Theory Tech.*, vol. 53, no. 11, pp. 3422–3428, Nov. 2005.

[45] J. C. Pedro and S. A. Maas, "A comparative overview of microwave and wireless power-amplifier behavioral modeling approaches," *IEEE Trans. Microw. Theory Tech.*, vol. 53, no. 4, pp. 1150–1163, Apr. 2005.

[46] M. Isaksson, D. Wisell, and D. Rönnow, "A comparative analysis of behavioral models for RF power amplifiers," *IEEE Trans. Microw. Theory Tech.*, vol. 54, no. 1, pp. 348–359, Jan. 2006.
[47] A. S. Tehrani, H. Cao, S. Afsardoost, T. Eriksson, M. Isaksson, and C. Fager, "A comparative analysis of the complexity/accuracy tradeoff in power amplifier behavioral models," *IEEE Trans. Microw. Theory Tech.*, vol. 58, no. 7, pp. 1510–1520, Jun. 2010.
[48] J. Vuolevi and T. Rahkonen, *Distortion in RF Power Amplifiers*. Norwood, MA: Artech House, 1999.
[49] J. Kim, Y. Y. Woo, J. Moon, and B. Kim, "A new wideband adaptive digital predistortion technique employing feedback linearization," *IEEE Trans. Microw. Theory Tech.*, vol. 56, no. 2, pp. 385–392, Feb. 2008.
[50] O. Hammi and F. M. Ghannouchi, "Twin nonlinear two-box models for power amplifiers and transmitters exhibiting memory effects with application to digital predistortion," *IEEE Microw. Wireless Compon. Lett.*, vol. 19, no. 8, pp. 530–532, Aug. 2009.
[51] S. Hong, Y. Y. Woo, J. Kim, J. Cha, I. Kim, J. Moon, J. Yi, and B. Kim, "Weighted polynomial digital predistortion for low memory effect Doherty power amplifier," *IEEE Trans. Microw. Theory Tech.*, vol. 55, no. 5, pp. 925–931, May 2007.
[52] L. Ding and G. T. Zhou, "Effects of even-order nonlinear terms on power amplifier modeling and predistortion linearization," *IEEE Trans. Veh. Technol.*, vol. 53, no. 1, pp. 156–162, Jan. 2004.
[53] "Connected simulation and test solutions using the Advanced Design System," Agilent Technol., Palo Alto, CA, Appl. Note 1394, 2000.
[54] B. B. Jovanovic, I. S. Reljin, and B. D. Reljin, "Modified ANFIS architecture-improving efficiency of ANFIS technique," *Neural Netw. Appl. Elect. Eng.*, pp. 215–220, Sep. 2004.
[55] D. Wisell, M. Isaksson, and N. Keskitalo, "A general evaluation criteria for power amplifier behavioral PA models," in *Proc. 69th ARFTG Conf. Dig.*, 2007, pp. 251–255.
[56] H. Ku and J. S. Kenney, "Behavioral modeling of nonlinear RF power amplifiers considering memory effects," *IEEE Trans. Microw. Theory Tech.*, vol. 51, no. 12, pp. 2495–2504, Dec. 2003.
[57] O. Hammi, S. Carichner, B. Vassilakis, and F. M. Ghannouchi, "Power amplifiers' model assessment and memory effects intensity quantification using memoryless post-compensation technique," *IEEE Trans. Microw. Theory Tech.*, vol. 56, no. 12, pp. 3170–3179, Dec. 2008.

Junghwan Moon (S'07) received the B.S. degree in electrical and computer engineering from the University of Seoul, Seoul, Korea, in 2006, and is currently working toward the Ph.D. degree at the Pohang University of Science and Technology (POSTECH), Pohang, Gyeongbuk, Korea.

His current research interests include highly linear and efficient RF PA design, memory-effect compensation techniques, DPD techniques, and wideband RF PA design.

Mr. Moon was the recipient of the Highest Efficiency Award of the Student High-Efficiency Power Amplifier Design Competition, 2008 IEEE Microwave Theory and Techniques Society (IEEE MTT-S) International Microwave Symposium (IMS).

Bumman Kim (M'78–SM'97–F'07) received the Ph.D. degree in electrical engineering from Carnegie Mellon University, Pittsburgh, PA, in 1979.

From 1978 to 1981, he was engaged in fiber-optic network component research with GTE Laboratories Inc. In 1981, he joined the Central Research Laboratories, Texas Instruments Incorporated, where he was involved in development of GaAs power field-effect transistors (FETs) and monolithic microwave integrated circuits (MMICs). He has developed a large-signal model of a power FET, dual-gate FETs for gain control, high-power distributed amplifiers, and various millimeter-wave MMICs. In 1989, he joined the Pohang University of Science and Technology (POSTECH), Pohang, Gyeongbuk, Korea, where he is a POSTECH Fellow and a Namko Professor with the Department of Electrical Engineering, and Director of the Microwave Application Research Center, where he is involved in device and circuit technology for RF integrated circuits (RFICs). He has authored over 300 technical papers.

Prof. Kim is a member of the Korean Academy of Science and Technology and the National Academy of Engineering of Korea. He was an associate editor for the IEEE TRANSACTIONS ON MICROWAVE THEORY AND TECHNIQUES, a Distinguished Lecturer of the IEEE Microwave Theory and Techniques Society (IEEE MTT-S), and an Administrative Committee (AdCom) member.